High-Power 50-GHz Double-Drift-Region IMPATT Oscillators with Improved Bias Circuits for Eliminating Low-Frequency Instabilities

YASUTAKE HIRACHI, MEMBER, IEEE, TAKAKIYO NAKAGAMI, MEMBER, IEEE, YOSHIKAZU TŌYAMA, AND YUKIO FUKUKAWA

Abstract—**Low-frequency instabilities in millimeter-wave double-drift-region (DDR) IMPATT diodes are investigated and new oscillator circuits with the improved bias circuits for eliminating the low-frequency instability are developed. DDR IMPATT diodes mounted in these circuits exhibited a maximum free-running oscillation power of 1.6 W at 55.5 GHz with 11.5-percent conversion efficiency. A highly stabilized oscillator was also constructed with the maximum output power of 1 W and the frequency stability 0.3 ppm/mA at 51.86 GHz.**

Introduction

THE double-drift-region (DDR) IMPATT diodes are presently considered as the only solid-state active device that can produce output power on the order of 1 W in the millimeter-wave range. It has been confirmed that the millimeter-wave output power and efficiency are significantly higher for DDR diodes than that obtained with the single-drift-region (SDR) IMPATT diodes [1]. DDR diodes, however, have not yet been practically utilized at their highest power and efficiency levels. The reason for this is that there still remain some problems to be solved in the practical utilization of DDR diodes. One of these problems is that DDR diodes are prone to low-frequency instabilities because of the high conversion efficiency [2].

Low-frequency instabilities in IMPATT diodes have a detrimental effect on microwave oscillation [3]. Low-frequency instabilities would result in excessive noise increase, tuning-induced diode burnout, and microwave output power decrease. These instabilities are more prominent in higher efficiency, higher power, and higher frequency diodes. That is, these phenomena are serious problems in millimeter-wave IMPATT diodes, especially in millimeter-wave DDR IMPATT diodes which have a high power capability. Therefore, the elimination of the low-frequency instability is essential in the practical utilization of millimeter-wave DDR diodes. One can expect that high-power millimeter-wave oscillators having low sideband noise can be obtained if this low-frequency instability is suppressed.

In this paper, the low-frequency instabilities in millimeter-wave DDR IMPATT diodes are investigated and the low-frequency impedance of DDR diodes is derived. It is shown that DDR diodes are more prone to instability than SDR diodes. Some new oscillator circuits with improved bias circuits for eliminating low-frequency instabilities are proposed. DDR IMPATT diodes mounted in these circuits exhibited output powers of 1.6 W at 55.5 GHz with 11.5-percent conversion efficiency. A highly stabilized oscillator was also constructed with the maximum output power of 1 W at 51.86 GHz and the frequency stability 0.3 ppm/mA.

Manuscript received February 23, 1976; revised May 10, 1976.
The authors are with Fujitsu Laboratories Ltd., Nakahara, Kawasaki 211, Japan.

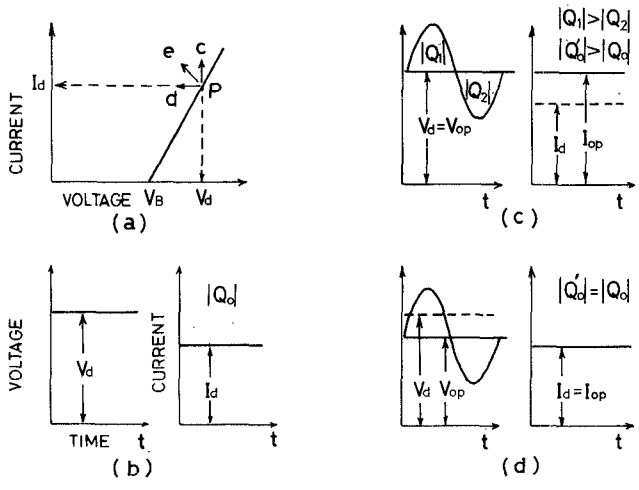

Fig. 1. Origins of the low-frequency negative resistance in the IMPATT diode. (a) Voltage–current characteristics of the reverse-biased IMPATT diode. (b) RF voltage amplitude $V_{RF} = 0$. $|Q_0|$ is the amount of the charge induced by avalanche. (c) $V_{RF} > 0$. The amount of charge $|Q_1|$ induced between 0 and π in the phase of RF voltage becomes larger than that of the charge $|Q_2|$ which is removed between π and 2π because of the excess increase of the charge induced by avalanche due to the extreme nonlinearity of the ionization coefficient. (d) $V_{RF} > 0$. When the constant current is applied to the diode, the operating voltage V_{op} decreases so as to satisfy the condition of $|Q_0'| = |Q_0|$, where $|Q_0'|$ is the amount of the charge induced by avalanche in case of $V_{RF} > 0$.

Origins of Low-Frequency Negative Resistance in IMPATT Diodes and Influences of the Low-Frequency Instability

Low-frequency negative resistance originates in the excessive increase of the charges induced by avalanche with increasing RF voltage amplitude V_{RF} due to the extreme nonlinearity of the ionization coefficient α as a function of the electric field E [4]. This mechanism is explained in more detail in Fig. 1. Fig. 1(a) shows the voltage–current characteristics of the reverse-biased IMPATT diode. At point P, in the case of $V_{RF} = 0$, the applied voltage V and

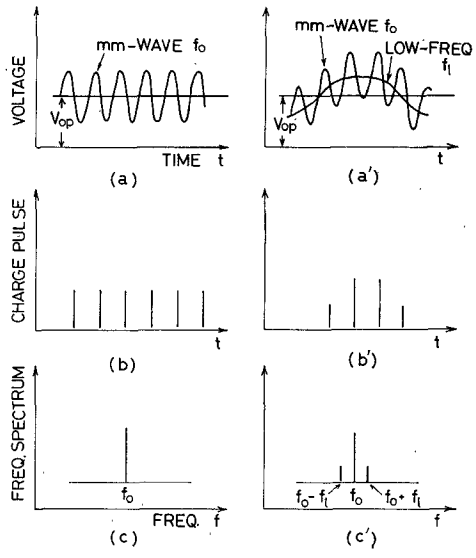

Fig. 2. The outline of the influence of the low-frequency instability on the IMPATT operation of the diode. The left-hand side represents the normal IMPATT oscillation and the right-hand side the anomalous oscillation where low-frequency instability appears.

the direct current I_d is constant with time, as shown in Fig. 1(b), where $|Q_0|$ is the amount of the charge induced by avalanche. With the RF voltage applied [in Fig. 1(c)], the amount of the charge $|Q_1|$ induced between 0 and π in the phase of the RF voltage becomes larger than that of the charge $|Q_2|$ removed between π and 2π due to the nonlinearity of α. That is, $|Q_1| > |Q_2|$ so that the amount of the charge $|Q_0'|$ induced in one cycle of the RF voltage is larger than $|Q_0|$. Then, if the applied voltage V_d is constant, the operating current I_{op} increases more than I_d [as shown in Fig. 1(a), arrow c]. If the constant current is applied to the diode [in Fig. 1(d)], the operating voltage V_{op} decreases so as to satisfy the condition of $|Q_0'| = |Q_0|$ [in Fig. 1(a), arrow d]. If both V_{op} and I_{op} are not constrained, V_{op} decreases and I_{op} increases with increasing V_{RF}, i.e., dV_{op}/dI_{op} is negative. This is the reason why the low-frequency negative resistance appears in IMPATT diodes.

The outline of the influence of low-frequency instability on the IMPATT operation is shown in Fig. 2. The left-hand side of Fig. 2 represents the normal IMPATT operation and the right-hand side the anomalous one where the low-frequency instability appears. When the low-frequency voltage amplitude superimposes on the millimeter-wave one, the phase and the amount of the charge pulse generated by avalanche will shift randomly, whereas a constant charge pulse train is generated in the π phase of the millimeter-wave voltage amplitude when the diode operates in the normal IMPATT mode. It is assumed from these speculations that the millimeter-wave output power will be reduced by the occurrence of the low-frequency oscillation.

Low-Frequency Impedance of DDR IMPATT Diodes and Elimination of Low-Frequency Instabilities

The equation representing the relation among the operating voltage V_{op}, the applied current I_d, and the RF voltage amplitude V_{RF} in SDR IMPATT diodes was first derived by Read [5]

$$V_{op} = R_{sc} I_d - \frac{m}{4WE_c} V_{RF}^2 + \text{constant} \qquad (1)$$

where R_{sc} is the space charge resistance, W is the depletion layer width, E_c is the critical field for avalanche breakdown, m is $(E_c/\alpha) \cdot (d\alpha/dE)|_{E_c}$, and α is the ionization coefficient.

A DDR diode has equal drift layers for holes and electrons. As these layers are arranged in series, the operating voltage V_{op} in the DDR diode is composed of the algebraic sum of the operating voltage $V_{op(p)}$ applied to p layer and $V_{op(n)}$ to n layer, i.e., $V_{op} = V_{op(p)} + V_{op(n)}$. Equations similar to (1) can be derived for p and n layers in DDR diodes. By adding two equations, we can have the following equation for DDR diodes:

$$V_{op} = R_{sc} I_d - \frac{m_n + m_p}{8WE_c} V_{RF}^2 + \text{constant} \qquad (2)$$

where m_n and m_p is $(E_c/\alpha_n) \cdot (d\alpha_n/dE)|_{E_c}$ and $(E_c/\alpha_p) \cdot (d\alpha_p/dE)|_{E_c}$, respectively, α_n and α_p are ionization coefficients for electron and hole, respectively, and W is the total active layer width in DDR diodes. In addition, the following assumptions have been made:

$$W_{(p)} = W_{(n)} = 1/2 \cdot W \qquad V_{op(p)} = V_{op(n)} = 1/2 \cdot V_{op}$$

$$V_{RF(p)} = V_{RF(n)} = 1/2 \cdot V_{RF} \qquad R_{sc(p)} + R_{sc(n)} = R_{sc}$$

where the suffixes (p) and (n) represent the p- and n-type layers, respectively.

Differentiating both sides of (2) with respect to I_d, we obtain

$$\frac{dV_{op}}{dI_d} = R_{sc} - \frac{m_n + m_p}{4WE_c} \cdot V_{RF} \cdot \left(\frac{dV_{RF}}{dI_d}\right). \qquad (3)$$

Using the relation $P_{out} = 1/2 \cdot |G_{op}| \cdot V_{RF}^2$, (3) can be written

$$\frac{dV_{op}}{dI_d} = R_{sc} - \frac{m_n + m_p}{4WE_c} \cdot \frac{1}{|G_{op}|} \cdot \left(\frac{dP_{out}}{dI_d}\right) \qquad (4)$$

where G_{op} is the operation conductance and P_{out} is the output power. If we define $dV_{op}/dI_d \equiv R_{DDR}$, R_{DDR} represents the low-frequency negative resistance of DDR diodes.

Brackett [3] derived the low-frequency impedance Z_{SDR} for SDR diodes given by

$$Z_{SDR} = R_{sc} - \frac{R_-}{1 + j\dfrac{\omega}{\gamma}} \qquad (5a)$$

$$R_- = \frac{m}{2WE_c} \cdot \frac{1}{|G_{op}|} \cdot \left(\frac{dP_{out}}{dI_d}\right) \qquad (5b)$$

where γ is a quantity associated with the saturation parameters of the large-signal behavior of the diode, the millimeter-wave oscillation frequency, and the loaded cavity Q [3]. The second term on the right-hand side of (4) is similar to (5b). Hence the low-frequency impedance Z_{DDR}

TABLE I
PHYSICAL DATA AND NEGATIVE RESISTANCE VALUES FOR MILLIMETER-WAVE Si-SDR AND -DDR IMPATT's

	Si SDR	Si DDR		Source
Diode	37-1H	39-16S		
Diode Capacitance Co (pF)	1.4	1.2		Measured
C breakdown (pF)	0.32	0.28		Measured
Junction Area S(cm^2)	1.6×10^{-5}	2.2×10^{-5}		Calculated
Series Resistance Rs(ohms)	1.06	0.85		Estimated[6]
Breakdown Voltage V_B(volts)	17.3	21.3		Measured
Depletion Layer Width W(microns)	0.72 at 23(V)	0.89 at 29(V)		Estimated
Critical Field Ec(volts/cm)	5.5×10^{-5}	4.7×10^{-5}		Estimated
$\frac{Ec}{\alpha}\left(\frac{d\alpha}{dE}\right)_{Ec}$	$\alpha_n = 1.38\times10^{5}(cm^{-1})$ $\alpha_n' = 9.20\times10^{-1}(V^{-1})$ $m_n = 3.67$	$\alpha_n = 9.20\times10^{4}(cm^{-1})$ $\alpha_p = 2.22\times10^{4}(cm^{-1})$ $\alpha_n' = 9.20\times10^{-1}(V^{-1})$ $\alpha_p' = 3.48\times10^{-1}(V^{-1})$ $m_n = 4.72$ $m_p = 7.40$		Calculated[4]
dPout/dId (watts/amp)	4.0	5.9		Measured
Negative Conductance Gop (mhos)	10.7×10 at 457 mW	S=$1.6\times10^{-5}cm^2$ 7.4×10^{-3}	S=$2.2\times10^{-5}cm^2$ 10.2×10^{-3} at 1023 mW	Measured with X Band Simulation Method(7)(8)
R_ (ohms)	17.3	57.5	41.7	Calculated
Rsc (ohms)	5.0	8.0	6.0	Measured
Low Frequency Negative Resistance at ω = 0 (ohms)	-12.3	-49.5	-35.7	Calculated
Loaded Cavity Q Q_L	30	38	38 / 400	Measured at Operating Frequency
Millimeter-wave Oscillation Frequency fo (GHz)	55.5	55.5	55.5 / 55.5	
Maximum Frequency f_{max}(GHz)	3.4	3.6	3.6 / 0.34	

of DDR diodes can be expressed by

$$Z_{DDR} = R_{sc} - \frac{R_-}{1 + j\frac{\omega}{\gamma}} \tag{6a}$$

$$R_- = \frac{m_n + m_p}{4WE_c} \cdot \frac{1}{|G_{op}|} \cdot \left(\frac{dP_{out}}{dI_d}\right). \tag{6b}$$

At $\omega = 0$, $Z_{DDR} = R_{DDR}$ and using each parameter of DDR (39-16S) as listed in Table I, R_{DDR} is calculated to be about $(-)$ 50 Ω, which is four times as large as R_{SDR}. This shows that these instabilities will be observed more frequently in DDR than in SDR.

We can derive from (6a) the maximum frequency f_m for which Z_{DDR} has a negative real part. The maximum frequency f_{max} is given by (see [3])

$$f_{max} = \frac{f_0}{Q_L}\sqrt{\frac{R_-}{R_{sc}} - 1} \tag{7}$$

where f_0 is the millimeter-wave oscillation frequency, and Q_L is the loaded cavity Q. The calculated value of $f_{max(DDR)}$ for DDR diodes (39-16S) using (7) is about 3.6 GHz as listed in Table I, while $f_{max(SDR)}$ for SDR diodes is about 3.4 GHz. Smith chart plots of $(-)$ Z_{DDR} and $(-)$ Z_{SDR} with the frequency ω are shown in Fig. 3(a) in the case where the junction area is 1.6×10^{-5} cm^2 for both SDR and DDR.

The f_{max} in millimeter-wave DDR diodes is several hundred times as large as that in microwave diodes. For example, the f_{max} is about 16 MHz in J-band GaAs IMPATT diodes [3]. The suppression of instabilities in higher frequency diodes is more difficult than in lower frequency diodes. Therefore, these phenomena are more prominent in higher frequency diodes.

The outline of the frequency dependence of the negative resistance which DDR (39-16S) can have is illustrated in Fig. 3(b). Region 1 shows the intrinsic negative resistance area of DDR diodes, where ω_a is the avalanche frequency. Region 2 shows the frequency band in which the RF voltage-induced negative resistance appears. The dotted line means that thermal effects become important and introduce further positive resistance. The low-frequency negative resistance (region 2) appears only when the millimeter-wave oscillation builds up (region 1). The load for this low-frequency negative resistance is the bias-circuit impedance seen from the diode. Therefore, in order to suppress the low-frequency instability in DDR diodes, we consider the following two methods (conditions):

1) A method for making the bias-circuit impedance extremely small ($\sim$ short circuit) compared with $(-)$ Z_{DDR} at frequencies in excess of $f_{min(DDR)}$ [see Fig. 3(b)] for the low-frequency instabilities.

2) A method for making the bias-circuit impedance greater than $(-)$ Z_{DDR} at frequencies lower than $f_{max(DDR)}$ for DDR. (This is the absolutely stable condition for low-frequency oscillation.)

In our experiments the low-frequency instability was observed to be prominent in the frequency range from 100 MHz[1] to 1 GHz. Therefore, if the bias-circuit impedance is kept small in this frequency range, condition 1) will be

[1] The thermal time constant should be of the order of at least 1 μs. However, the f_{min} in our experiments was about 100 MHz of which time constant was 1/100 μs. The reason why this discrepancy occurs is still unclear.

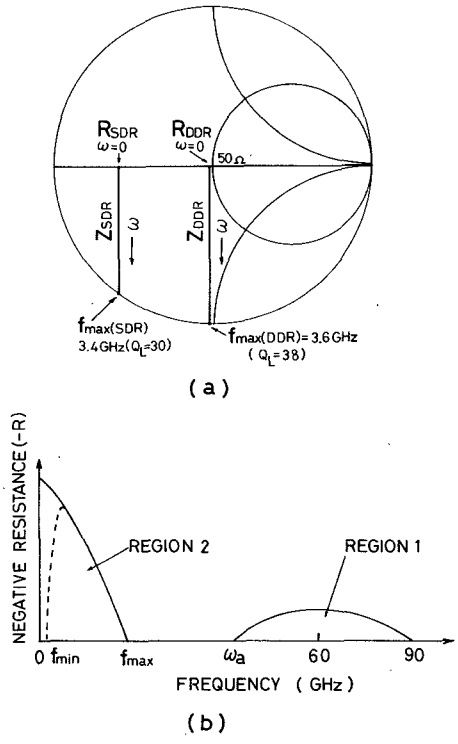

Fig. 3. (a) Smith chart plots of the low-frequency impedance $(-)Z_{DDR}(\omega)$ and $(-)Z_{SDR}(\omega)$ for DDR and SDR IMPATT diodes, respectively. Equation (6) gives a slight curve on the Smith chart when normalized by $Z_0(= 50\ \Omega)$ and gives a straight vertical line when normalized by R_{sc} (which is usually smaller than 50 Ω). In this case, for simplicity, (6) has been drawn as the straight vertical line even if normalized by $Z_0(= 50\ \Omega)$. It does not influence the result of this discussion. The junction area is 1.6×10^{-5} cm² for both SDR and DDR. (b) Negative resistance of DDR diodes versus the frequency. Region 1 shows the intrinsic negative resistance area of DDR diodes, where ω_a is the avalanche frequency. Region 2 shows the frequency band of the RF voltage-induced negative resistance. The dotted line means that in a very-low-frequency band, thermal effects become important and introduce further positive resistance. The low-frequency negative resistance appears only when the millimeter-wave frequency oscillation builds up.

satisfied. It is seen from Fig. 3(a) that suppressing the instability in DDR diodes is more difficult than in SDR diodes, since Z_{DDR} and $f_{max(DDR)}$ are greater than Z_{SDR} and $f_{max(SDR)}$, respectively.

Bias-Circuit Impedance of the Conventional Coaxial-Waveguide Circuit and Cap-Type Circuit

The bias-circuit impedance $Z_B(\omega)$ seen from the diode was measured with a network analyzer and a small coaxial probe with $Z_0 = 50\ \Omega$ [9], in place of the diode. Fig. 4(b) shows the bias-circuit impedance locus $Z_{B1}(\omega)$ of the conventional coaxial-waveguide circuit as illustrated in Fig. 4(a), which has been used in millimeter-wave communication systems [10]. It is seen from Fig. 4(b) that the $Z_{B1}(\omega)$ locus intersects the $(-)Z_{DDR}$ locus within frequencies from several tens of megahertz to about 1 GHz. In this frequency band the low-frequency instabilities have been experimentally observed to be more prominent. The junction area of the diode used in this experiment is 2.2×10^{-5} cm² (see Table I). Fig. 5 shows the impedance locus of the same circuit as that of Fig. 4(a) except for the insertion of a parallel circuit of a resistor ($R \sim 500\ \Omega$) and

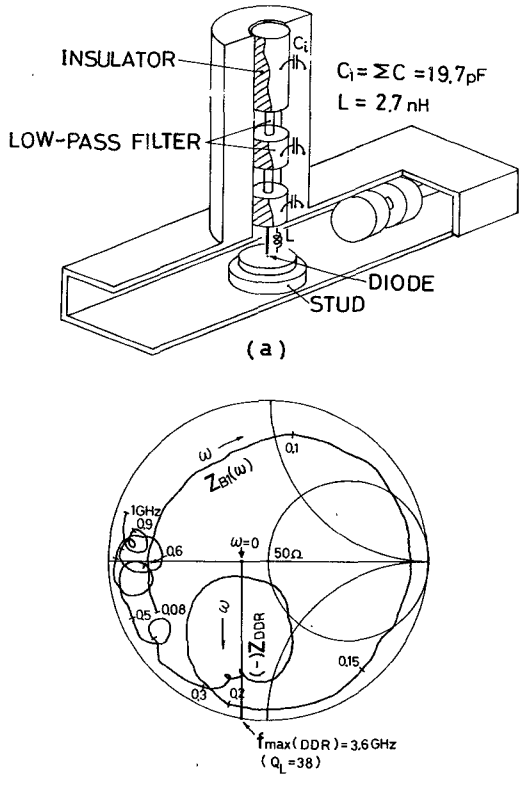

Fig. 4. (a) Coaxial-waveguide circuit used in millimeter-wave communication systems [10]. (b) The bias-circuit impedance locus of this circuit. The $Z_{B1}(\omega)$ locus intersects the $(-)Z_{DDR}(\omega)$ locus. The junction area of the diode used in this experiment is 2.2×10^{-5} cm².

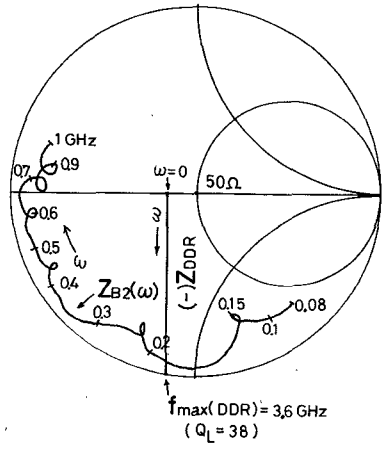

Fig. 5. The bias-circuit impedance locus $Z_{B2}(\omega)$ of the same circuit as that of Fig. 4(a), except for the insertion of a parallel circuit of a resistor ($R \sim 500\ \Omega$) and an inductor ($L \sim 23\ \mu$H).

an inductor ($L \sim 23\ \mu$H) in series with the dc bias feed line between the diode cavity and the dc power supply. The $Z_{B2}(\omega)$ locus is simpler at frequencies below 0.3 GHz than that of Fig. 4(b). But as this locus also intersects the $(-)Z_{DDR}(\omega)$ locus, no improvement can be expected for the low-frequency instability. At 0.65 GHz, the $Z_{B2}(\omega)$ locus intersects the line of $jX = 0$. The reason for this is that the capacitance C_1 [$\sim$ 19.7 pF, see Fig. 4(a)] and inductance L of the inner conductor in the coaxial line are in series

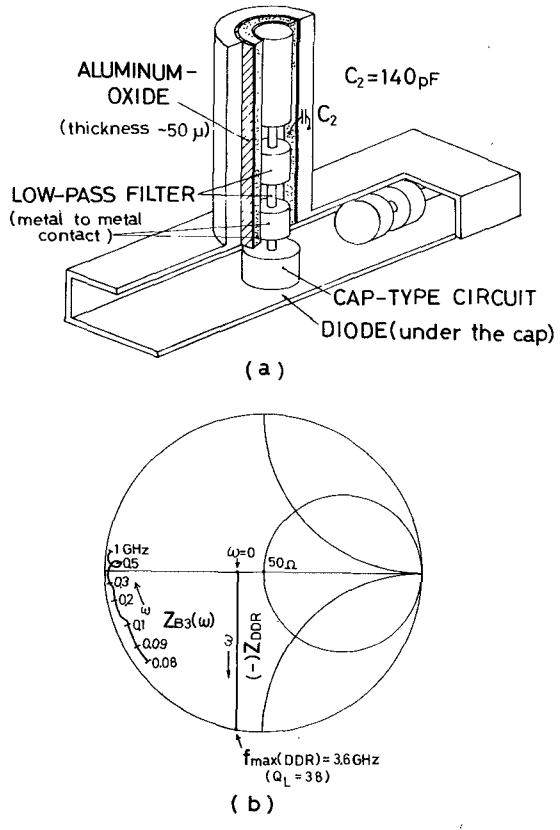

Fig. 6. (a) Improved cap-type circuit. A large capacitance (~ 140 pF) made of aluminum oxide (thickness ~ 50 μm) is placed so as to surround the low-pass filter. (b) The bias-circuit impedance locus Z_{B3} (ω) of this circuit. Compared with Fig. 5, the impedance is successfully kept low at frequencies in excess of 80 MHz.

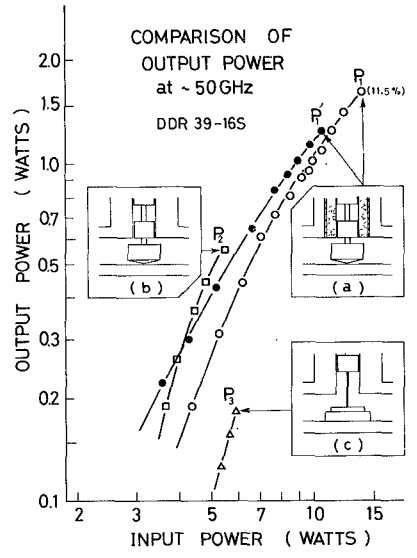

Fig. 7. Output power and conversion efficiency versus input power for typical devices mounted in the three kinds of circuits. The junction area of the diodes used is about 2.2 × 10^{-5} cm^2 and the typical value of the thermal resistance of these diode is about 25°C/W. (a) ∧ : improved cap-type circuit. Maximum power and efficiency obtained is ~ 1.6 W and 11.5 percent, respectively. (b) □: unimproved cap-type circuit. The low frequency instability occurred at P_2. (c) △: conventional coaxial-waveguide circuit. The low-frequency instability occurred at P_3.

resonance at 0.65 GHz. The inductance L calculated from $L = 1/\omega^2 C$ is about 2.7 nH, which is in reasonable agreement with the calculated value of 1.8 nH. It may be concluded that due to the capacitance of the low-pass filter, the $Z_{B2}(\omega)$ locus represents the negative reactance at lower frequencies than 0.65 GHz.

As the millimeter-wave circuit satisfying condition 2) can not be easily constructed because of the very small dimensions, we first tried to realize method 1). In order to realize method 1), it is necessary to remove inductance L and to put a large capacitance in the vicinity of the diode. Therefore, a millimeter-wave circuit having an inductance near the diode, such as a coaxial-waveguide type, is not suitable for DDR IMPATT diodes. From this point of view, the cap-type circuit might be preferable for DDR diodes as it has no inductance near the diode. The bias-circuit impedance locus of the unimproved cap-type circuit, with the parallel circuit in the dc bias feed line at frequencies lower than 0.65 GHz, was observed to be similar to that of Fig. 5. Under this condition the low-frequency instability would not be suppressed. It is necessary to improve the cap-type circuit so as to satisfy condition 1). In order to make the bias-circuit impedance extremely small without producing any loss in millimeter-wave power and efficiency, a large capacitance (C_2 ~ 140 pF) made of aluminum oxide (thickness 50 μm) was placed so as to surround the low-pass filter as illustrated in Fig. 6(a). The bias-circuit impedance locus $Z_{B3}(\omega)$ of this circuit is shown in Fig. 6(b). Compared with Fig. 5, the impedance was successfully kept low at frequencies in excess of 80 MHz. It is expected that the low-frequency instability will not build up in this circuit configuration.

Experimental Results and Practical Design Considerations

The fabrication technique of diodes used in microwave measurements is the following: The diode pellet was mounted on a diamond heat sink and the junction area was controlled to be about 2.2 × 10^{-5} cm^2 by chemical etching. The typical value of the thermal resistance of these diodes is 25°C/W. The contact resistance of these diodes is fully reduced by forming the n^{++} (~ 10^{20} cm^{-3}) layer near the surface of the n^+ substrate by arsenic ion implantation [6].

Fig. 7 shows the output power and conversion efficiency versus the input power for typical devices mounted in the three kinds of circuits. In the case of the conventional coaxial-waveguide circuit as illustrated in insert (c), the oscillation frequency spectrum observed with the spectrum analyzer showed a large amount of sideband noise and the output power obtained was at most 200 mW. Next, using the unimproved cap-type circuit as illustrated in insert (b), the maximum output power obtained was 500 mW. When the input power was further increased, the low-frequency instability occurred and the output power did not increase any more.

In the case of the improved cap-type circuit as illustrated in insert (a), power and efficiency as high as 1.6 W (point P_1) and 11.5 percent, respectively, were achieved at 55.5 GHz, which is the best power times frequency squared product (pf^2) reported so far for any microwave solid-state

devices. At this power level, no degradation in frequency spectrum was observed. When the bias current was further increased, the diode burned out.

It is evident that DDR IMPATT diodes can exhibit their intrinsic high-power characteristics if the low-frequency instabilities are suppressed. In order to use these diodes in a practical system, it is necessary that the low-frequency instabilities be completely eliminated under every operating condition. This requires that the bias circuit be designed by method 2) to satisfy the absolutely stable condition. In addition, the circuit should be easily designed to operate the DDR IMPATT diodes at any specified frequency with the maximum power. The improved cap-type circuit described previously is not suitable for this purpose, because a slight change of bias current or load impedance will cause low-frequency instabilities at a high output power level. Furthermore, the design of the cap-type circuit for a specific frequency is not easy. Therefore, it is necessary to develop a new millimeter-wave oscillator circuit suitable for the practical application of DDR IMPATT diodes.

In order to construct a circuit which satisfies the absolutely stable condition, the bias-circuit impedance must be greater than $(-)$ Z_{DDR} in the frequencies below $f_{max(DDR)}$. For this purpose, either or both of the following conditions should be realized:

1) To make the circuit Q (Q_L) so large that $f_{max(DDR)}$ becomes lower than the frequency at which the $Z_B(\omega)$ locus intersects the $(-)$ Z_{DDR} locus.

2) To remove the capacitance in the vicinity of the diode and to insert an inductance or a parallel circuit of L and R in some place of the millimeter-wave circuit without affecting the millimeter-wave oscillation.

Brackett [3] has proposed that the low-frequency instability of a 6-GHz GaAs IMPATT could be eliminated by inserting a resistive choke stabilizing network in a bias feed coaxial post immediately above the diode. In the millimeter-wave range, however, because of the very small dimensions of the circuit, this method cannot be used successfully and results in the large degradation of the millimeter-wave power and efficiency.

Cavity-Stabilized DDR Oscillator

From the aforementioned design considerations, the oscillator circuit shown in Fig. 8(a) was developed for 50-GHz-band applications using a WR-19 waveguide. A coaxial termination is incorporated in the bias circuit to give a high impedance loading to the diode in the frequency range of instabilities. To minimize the millimeter-wave dissipation, a radial line cavity band rejection filter is placed in the bias circuit. A high Q cylindrical cavity is placed in the waveguide circuit to increase the circuit Q of the oscillator. Millimeter-wave absorbers in the bias circuit and in the waveguide circuit are employed to suppress the spurious millimeter-wave oscillations. Impedance matching between the diode and the waveguide is made by a quarter-wave coaxial transformer which contacts the standoff of the diode. The oscillation frequency is determined by the geometry of this transformer and precise tuning can be made by the cylindrical cavity.

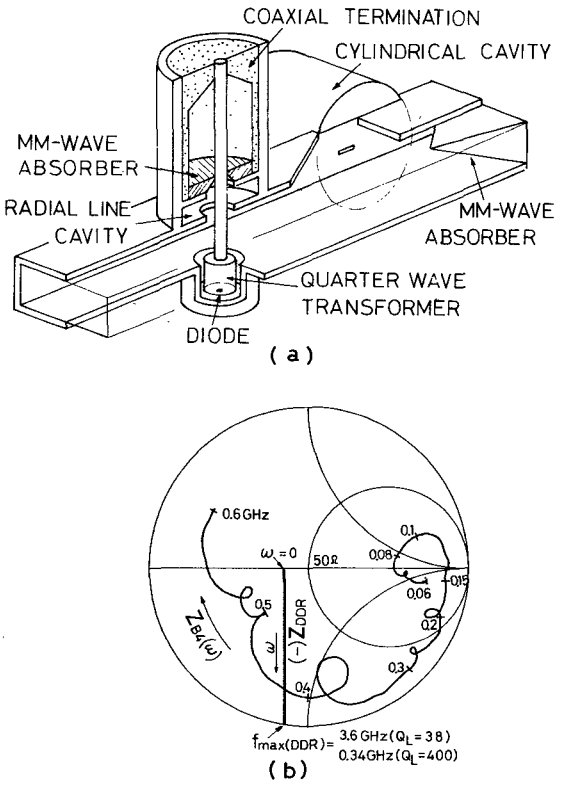

Fig. 8. (a) Cavity-stabilized DDR oscillator. The bias circuit provides a high-impedance coaxial termination to damp the instability. (b) The bias-circuit impedance locus of this circuit. The Z_{B4} locus intersects the $(-)$ $Z_{DDR}(\omega)$ locus at 0.42 GHz.

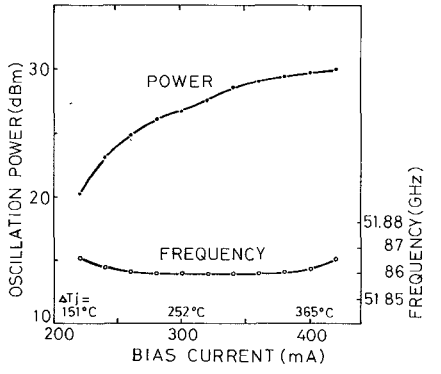

Fig. 9. Output power and oscillation frequency versus bias current for the highly stabilized DDR oscillator shown in Fig. 8(a). Maximum output power obtained is 1 W with the frequency stability less than 3 MHz over a 200-mA bias current range at 51.86 GHz.

The measured bias-circuit impedance of this circuit is shown in Fig. 8(b). It intersects the locus of $(-)$ Z_{DDR} at 0.42 GHz. Compared with the impedance diagram of Fig. 5, it is seen that this bias circuit is more stable against instabilities than that of Fig. 4(a). However, this bias circuit cannot satisfy the absolutely stable condition in the case of a free-running oscillator, where a waveguide short is connected instead of the cylindrical cavity and the absorber. In this case the circuit Q_L is 38 and $f_{max(DDR)}$ is about 3.6 GHz as shown in Fig. 8(b). In order to make the circuit Q_L higher, a cylindrical cavity has been incorporated and, as a result, the oscillator Q becomes as high as 400 and $f_{max(DDR)}$ is decreased to 0.34 GHz as listed in Table I.

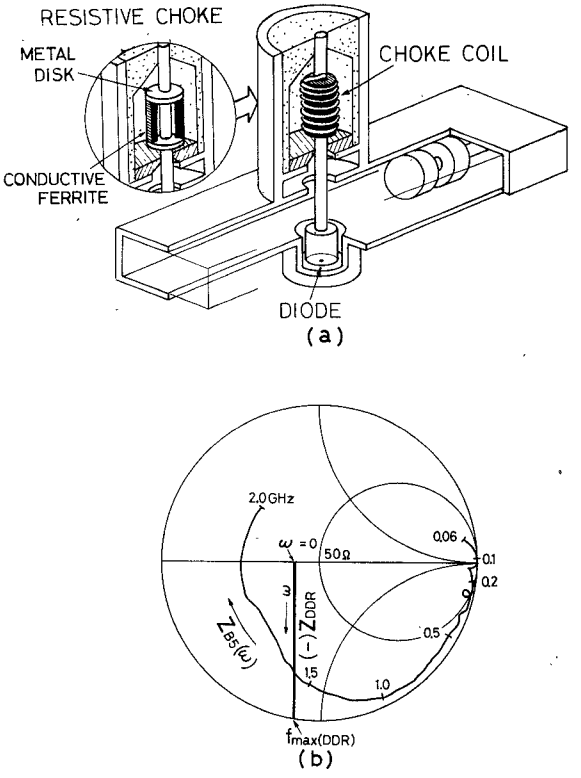

Fig. 10. (a) Modified bias circuit. An RF choke made of a thin wire and a ferrite core is inserted in the center conductor. Insert: Resistive choke which is composed of the lossy conductive ferrite (TDK-X502-RH) and the metal disk. (b) The bias-circuit impedance locus Z_{B5} of the circuit using an RF choke. Compared with Fig. 8(b), the impedance has been made fully large at frequencies lower than about 1 GHz.

Thus the f_{max} is made lower than the frequency of intersection at 0.42 GHz and the circuit is made stable.

Fig. 9 shows the performance of the developed DDR oscillator with the oscillation frequency of 51.86 GHz. The maximum output of 1 W was achieved at the bias current of 420 mA. The deviation of oscillation frequency was less than 3 MHz within a bias-current range from 220 to 420 mA. This gives a stability factor of 0.3 ppm/mA. Degradation of the oscillation frequency spectrum due to bias-current instabilities was not observed at any bias-current level.

In order to suppress the bias-circuit instability in free-running DDR oscillators without using a high Q cavity, it is necessary to modify the bias circuit so that the intersecting frequency between the two impedance loci is higher than $f_{max(DDR)}$. Fig. 10(a) shows an example of this scheme. In this circuit, an RF choke made of a thin wire and a ferrite core is inserted in the center conductor. In this configuration, the low-frequency range of instabilities is rejected by the RF choke and the high-frequency range is absorbed in the high impedance coaxial termination. Consequently, the bias-circuit impedance is made high to satisfy the absolutely stable condition. The measured bias-circuit impedance is shown in Fig. 10(b) when the inductance of RF choke was 5 μH. Compared with the impedance diagram of Fig. 8(b), it is seen that a drastic improvement is accomplished in the bias-circuit impedance, and low-frequency instabilities will not occur when $f_{max(DDR)}$ is less than 1.5 GHz.

Another method of realizing the resistive choke is also illustrated in the insert in Fig. 10(a). In this method a small tube of lossy conductive ferrite (TDK-X502-RH) is put around the center conductor. The equivalent circuit of this network is a parallel connection of the resistor ($R \sim 500\ \Omega$) and the inductor ($L \sim 0.04\ \mu$H). This method has a simpler construction than that using the thin wire and so it is more suitable for millimeter-wave oscillators. It is estimated that free-running DDR oscillators will be operated at their maximum output power without low-frequency instabilities by using these very small stabilizing networks.

Conclusion

The low-frequency instabilities in millimeter-wave DDR IMPATT diodes have been investigated. The equation representing the low-frequency impedance of DDR diodes has been derived. It has been shown that DDR diodes are more prone to instability than SDR diodes. New oscillator circuits with bias-circuit configurations for eliminating the low-frequency instability are proposed. The DDR diodes mounted in these circuits exhibited a maximum oscillation power of 1.6 W at 55.5 GHz with 11.5-percent efficiency. A frequency-stabilized oscillator has also been constructed with maximum output power of 1 W and frequency stability less than 0.3 ppm/mA at 51.86 GHz. It was shown that, by eliminating the low-frequency instability, millimeter-wave DDR IMPATT diodes can practically generate high power with high efficiency.

Acknowledgment

The authors wish to thank Dr. T. Kojima, Dr. T. Oshida, Dr. T. Misugi, Dr. M. Shinoda, and Mr. Tokoyo for their encouragement during this study, H. Nishi for the ion implantation, Y. Takeda for the millimeter-wave measurements, and S. Shibata for fabricating diodes.

References

[1] T. E. Seidel, R. E. Davis, and D. E. Iglesias, "Double-drift region ion-implanted millimeter-wave IMPATT diodes," *Proc. IEEE*, vol. 59, pp. 1222–1228, August 1971.
[2] Y. Hirachi, Y. Tōyama, Y. Fukukawa, and Y. Tokumitsu, "A high power 50 GHz DDR IMPATT oscillator with low side band noise," *Digest of 1976 MTT-S International Microwave Symposium*, June 1976.
[3] C. A. Brackett, "The elimination of tuning-induced burnout and bias-circuit oscillations in IMPATT oscillators," *Bell Syst. Tech. J.*, vol. 5, pp. 271–306, March 1973.
[4] S. M. Sze, *Physics of Semiconductor Devices*. New York: John Wiley, 1969.
[5] W. T. Read, "A proposed high-frequency negative resistance diode," *Bell Syst. Tech. J.*, vol. 37, pp. 401–446, March 1958.
[6] Y. Hirachi, H. Nishi, M. Shinoda, and Y. Fukukawa, "Millimeter-wave IMPATT diodes with improved efficiency by using ion-implanted ohmic contact," *Proc. IEEE* (Lett.), vol. 63, pp. 1367–1368, Sept. 1975.
[7] Y. Hirachi, Y. Tōyama, and M. Shinoda, "Frequency characteristics of IMPATTS," *Fujitsu Scientific and Tech. J.*, vol. 10, no. 3, pp. 105–122, 1974.
[8] H. Hayashi, F. Iwai, T. Fujita, M. Akaike, and H. Kato, "80 GHz IMPATT Amplifier," *ISSCC Digest of Technical Papers*, pp. 102–103, Feb. 1974.
[9] H. Komizo, Y. Itō, H. Ashida, and M. Shinoda, "A 0.5-W CW IMPATT diode amplifier for high-capacity 11-GHz FM radio relay equipment," *IEEE Trans. JSSC*, vol. 8, pp. 14–20, Feb. 1973.
[10] T. Miyakawa, N. Tokoyo, T. Nakagami, and H. Hayashi, "Wide-band tunable and highly stabilized millimeter-wave IMPATT diode oscillators," *Digest of 1975 MTT-S International Microwave Symposium*, pp. 222–223, May 1975.